Pneumococcal Trafficking across the Blood-Brain Barrier

Molecular Analysis of a Novel Bidirectional Pathway

Axel Ring,* Jeffrey N. Weiser,‡ and Elaine I. Tuomanen*

**Department of Infectious Diseases, St. Jude Children's Research Hospital, Memphis, Tennessee 38105; and ‡Department of Pediatrics and Department of Microbiology, Children's Hospital of Philadelphia and University of Pennsylvania Medical School, Philadelphia, Pennsylvania 19104*

Abstract

Although *Streptococcus pneumoniae* is a major cause of meningitis in humans, the mechanisms underlying its traversal from the circulation across the blood-brain barrier (BBB) into the subarachnoid space are poorly understood. One mechanism might involve transcytosis through microvascular endothelial cells. In this study we investigated the ability of pneumococci to invade and transmigrate through monolayers of rat and human brain microvascular endothelial cells (BMEC). Significant variability was found in the invasive capacity of clinical isolates. Phase variation to the transparent phenotype increased invasion as much as 6-fold and loss of capsule ~ 200-fold. Invasion of transparent pneumococci required choline in the pneumococcal cell wall, and invasion was partially inhibited by antagonists of the platelet-activating factor (PAF) receptor on the BMEC.

Pneumococci that gained access to an intracellular vesicle from the apical side of the monolayer subsequently were subject to three fates. Most opaque variants were killed. In contrast, the transparent phase variants were able to transcytose to the basal surface of rat and human BMEC in a manner dependent on the PAF receptor and the presence of pneumococcal choline-binding protein A. The remaining transparent bacteria entering the cell underwent a previously unrecognized recycling to the apical surface. Transcytosis eventually becomes a dominating process accounting for up to 80% of intracellular bacteria. Our data suggest that interaction of pneumococci with the PAF receptor results in sorting so as to transcytose bacteria across the cell while non-PAF receptor entry shunts bacteria for exit and reentry on the apical surface in a novel recycling pathway. (*J. Clin. Invest.* 1998. 102:347–360.) Key words: *Streptococcus pneumoniae* • endothelial cells • transmigration • adhesins • endocytosis

Introduction

Bacterial meningitis is the most serious infection of early childhood. It is typically preceded by sustained bacteremia with one of three high-grade pathogens, *Streptococcus pneumoniae, Haemophilus influenzae,* and *Neisseria meningitidis,* which localize to and cross the blood-brain barrier (BBB)[1] into the subarachnoid space. The unique capabilities shared by these bacteria which target them for interaction with and then allow them to penetrate the impervious intercellular tight junctions characteristic of the BBB are largely unknown. Anatomically, the BBB consists of different sites such as the cerebral capillary endothelium, the choroid plexus epithelium, and the arachnoid membrane. We selected the most extensive site, the brain microvascular endothelium, for our study. *Escherichia coli* use several fimbrial proteins to adhere to brain endothelial cells (1) and two specialized membrane proteins to invade brain microvascular endothelial cells (BMEC) (2, 3). However, susceptibility to this infection is limited to neonates, suggesting that different mechanisms may be operative for the childhood form of meningitis. Significant new information has been gathered for the molecular mechanism of adherence and invasion of lung epithelial and systemic endothelial cells by *S. pneumoniae*. Previous in vitro studies revealed that *S. pneumoniae* initially attaches to peripheral vascular endothelial cells via two classes of glycoconjugates whose minimal units consist of mannose linked to the disaccharides GalNAc β1-4 Gal or GalNAc β1-3 Gal (4, 5). Invasion of human endothelial cells is promoted by cytokine activation, which increases the amount of surface-expressed platelet-activating factor (PAF) receptor that in turn binds the phosphorylcholine component of the pneumococcal cell wall (6). In vitro experiments showed that invasion of unstimulated peripheral endothelial cells by *S. pneumoniae* is low (ratio of internalized to adherent bacteria $< 0.1\%$) whereas, in cytokine-activated cells, 2–3% of the adherent bacteria move to an intracellular compartment (6). Attenuation of inflammation or administration of PAF receptor antagonists (PAF-Ra) blocked the course of invasion from lung into blood in a rabbit model of pneumonia (6). These findings suggested that a working model for the transition from benign pneumococcal colonization of cell surfaces to invasive disease might include a step dependent on activation of host cells and subversion of the trafficking of the PAF receptor to promote bacterial translocation.

On the bacterial side of the invasive interaction, pneumococcal adherence to all cell types has been shown in vivo and in vitro to be affected by reversible phase variation marked by changes in colonial morphology from opaque to transparent. Both variants adhere to resting host cells, but only the transparent phenotype binds to the PAF receptor of activated cells

Address correspondence to Elaine I. Tuomanen, Department of Infectious Diseases, St. Jude Children's Research Hospital, 332 North Lauderdale Street, Memphis, TN 38105. Phone: 901-495-3486; FAX: 901-495-3099; E-mail: elaine.tuomanen@stjude.org

Received for publication 5 December 1997 and accepted in revised form 2 June 1998.

J. Clin. Invest.

0021-9738/98/07/0347/14 $2.00
Volume 102, Number 2, July 1998, 347–360
http://www.jci.org

1. *Abbreviations used in this paper:* BBB, blood-brain barrier; BMEC, brain microvascular endothelial cells; Cbp, choline-binding protein; LDH, lactate dehydrogenase; PAF, platelet-activating factor; PAF-Ra, PAF receptor antagonist; TEER, transendothelial electrical resistance.

(6, 7) and successfully colonizes the nasopharynx of infant rats (8). Once beyond the nasopharynx, opaque variants are more efficient at establishing bacteremia (9). A molecular explanation for these divergent capabilities has begun to emerge from an appreciation of the biochemical differences between the phenotypic variants. The transparent bacteria harbor more cell wall phosphorylcholine, less capsular polysaccharide, and bear different proteins on their surfaces than the opaque (8–10). Of particular interest, the transparent, invasive bacteria harbor significantly greater amounts of a newly described pneumococcal adhesin, choline-binding protein A (CbpA) (11). CbpA is presented on the pneumococcal surface via a noncovalent association with the choline of the cell wall and appears to promote increased pneumococcal attachment to activated human cells. Thus, in comparison to noninvasive opaque forms, transparent bacteria present more cell wall choline, the natural ligand for the PAF receptor (6), and more CbpA, a protein interacting with activated cells, a combination that favors invasion.

We sought to address directly how *S. pneumoniae* targets the brain resulting in the transition from bacteremia to infection of the subarachnoid space. Since *S. pneumoniae* bacteremia does not lead to meningitis in adult animal models, we chose to establish an in vitro model of the BBB using rat and human BMEC. We mapped the routes of bacterial trafficking into, out of, and across an in vitro model of the BBB and established the requirements for sorting bacteria into the various compartments in terms of phase variation, capsular polysaccharide, phosphorylcholine, CbpA, and PAF receptor. This study represents the first molecular description of the mechanism of invasion of the central nervous system by a high-grade pathogen of childhood.

Table I. Invasion of Rat BMEC by Clinical S. pneumoniae Isolates

Strain no.	Isolated from	Phase variant	Capsule type	Intracellular bacteria/well	T/O ratio	*P* value
P378	Blood	Opaque	9V	< 5		
P379	Blood	Transparent	9V	17±7	5.8	0.0035
P256	CSF	Opaque	6B	22±6		
P68	CSF	Opaque	18C	28±11		
P70	CSF	Transparent	18C	38±13	1.4	NS
P382	Blood	Opaque	6B	28±16		
P383	Blood	Transparent	6B	119±20	4.3	0.0001
P71	Blood	Opaque	18C	92±19		
P73	Blood	Transparent	18C	604±100	6.6	0.00004
P28	Blood	Opaque	7F	92±35		
P284	Blood	Opaque	7F	107±36		
P62	Blood	Opaque	9V	142±57		
P64	Blood	Transparent	9V	204±68	1.4	0.007
P373	Blood	Opaque	6A	218±58		
P374	Blood	Transparent	6A	308±65	1.4	0.022
P45	CSF	Mixed	18C	846±217		
P15	Blood	Mixed	19F	< 5		
P27	Blood	Mixed	7F	219±51		

Opaque/transparent pairs of the same original isolate are listed together. The values given are means and standard deviations of the number of intracellular CFU after 2 h of incubation with rat BMEC and antibiotic killing of extracellular CFU. For phase variant pairs, the T/O ratio of invasion (transparent divided by opaque) and the *P* value of the differences between opaque and transparent are given. *NS*, not significant ($P > 0.05$).

Methods

Preparation of bacteria. The clinical *S. pneumoniae* isolates presented in Table I were obtained from Dr. Robert Austrian (University of Pennsylvania). All isolates were confirmed to be encapsulated by Quellung reaction. The nonencapsulated strains P125 and P126 are phenotypic variants of R6, which is an unencapsulated laboratory-adapted isogenic derivative of an isolate of pneumococcus type 2 (10). The mutant in which the gene encoding CbpA was interrupted was generated in R6 as described (12). Streaking out on tryptic soy agar plates containing catalase as described (8) separated transparent and opaque phase variants. For invasion assays, pneumococci were grown overnight from frozen stocks on tryptic soy agar plates (Difco Laboratories, Detroit, MI) containing 3% defibrinated sheep blood (Micropure Medical, Inc., White Bear Lake, MN) in a 5% CO_2 atmosphere. Single colonies were inoculated into the semisynthetic medium C + Y (13) and grown to midlogarithmic phase ($OD_{620} = 0.4$). Quantitation of capsular polysaccharide and teichoic acid was carried out as previously described (9).

BMEC. Immortalized rat and human BMEC were used in this study. The rat brain microvessel-derived endothelial cell line EC 219 was generously provided by L. Juillerat (Institute of Pathology, University of Lausanne, Lausanne, Switzerland). The characterization and culture conditions of this cell line have been described (14, 15). The cells form a confluent monolayer displaying a cobblestone appearance when grown on collagen-coated surfaces, express Factor VIII–related antigen, angiotensin-converting enzyme, and alkaline phosphatase, and take up acetylated LDL. Their cerebral origin was confirmed by the expression of γ-glutamyltranspeptidase. We confirmed that these markers were expressed under our culture conditions. The cells were grown in DME supplemented with 10% FBS.

Transformed human BMEC from a brain biopsy of an adult female with epilepsy were a kind gift from Kwang Sik Kim (Children's Hospital of Los Angeles, Los Angeles, CA). These cells have been used recently to investigate the transmigration of *Streptococcus agalactiae* across a BBB in vitro model (16). They express Factor VIII–related antigen, carbonic anhydrase IV, and *Ulex europaeus* agglutinin I and take up acetylated LDL. Like the rat cells, human BMEC also express γ-glutamyltranspeptidase, thus proving their brain endothelial cell properties.

Both rat and human BMEC exhibit circumferential staining for the tight junction protein ZO-1 (as assessed by immunofluorescence, not shown) and enrichment of filamentous actin in the cell borders (demonstrated by rhodamine-phalloidin staining, not shown). The transendothelial electrical resistance (TEER) across BMEC monolayers grown on a collagen-coated Transwell filter (Corning Costar Corp., Cambridge, MA) was measured using the Millicell-Electrical Resistance System (Millipore, Bedford, MA). The TEER of rat BMEC is $\sim 125\ \Omega \times cm^2$, whereas human BMEC monolayers acquire a TEER of $\sim 200\ \Omega \times cm^2$.

Endothelial cell invasion assay. Invasion of BMEC was assayed by an antibiotic protection assay (17, 18) modified for *S. pneumoniae* (19). Pneumococcal cultures grown in C + Y to an OD_{620} of 0.4 were centrifuged and resuspended in DME plus 1% FBS at a concentration of $\sim 10^7$ CFU/ml according to Klett-Summerson photometer readings. The concentration was retroactively confirmed by viable counting on TSA blood plates. Confluent monolayers of BMEC grown in 24-well plates and control wells without cells were infected with 1-ml aliquots of bacterial suspension and incubated at 37°C. The concentration of bacteria in the supernatant fluid after 2 h was determined to evaluate bacterial replication. After 2 h (unless otherwise stated), the monolayers were washed three times with PBS. 1 ml of

DME + 1% FBS supplemented with penicillin G (10 μg/ml) and gentamicin (200 μg/ml) was added to each well and remained there for 1 h to kill all extracellular bacteria. Controls were performed to ensure that the antibiotic concentrations used were sufficient to kill 10^8 CFU/ml in 1 h. The monolayers were then washed three times again and detached from the surface by 200 μl 0.25% trypsin/0.02% EDTA. Cells were lysed by addition of 800 μl 0.025% ice-cold Triton X-100 and 100-μl aliquots were plated on tryptic soy agar plates containing 3% sheep blood to determine the total number of intracellular bacteria. To determine the total number of bacteria, both adherent and intracellular, infected monolayers were incubated for 30 min with bacteria, then washed, detached, and lysed as described above without antibiotic treatment. All assays were performed in four to six parallel wells and at least three independent experiments. Results of representative experiments are presented as mean±standard deviation. The significance of the difference between means was determined using the unpaired two-tailed Student's *t* test.

Recycling and transcytosis assay. To measure recycling and transcytosis of pneumococcus through BMEC, a double chamber culture system was set up using Transwell polycarbonate membrane filters (12 μm pore size, Cat. No. 3403; Corning Costar Corp.) placed into 12-well tissue culture plates (Fig. 1). The polycarbonate membranes were coated with collagen (Collagen R; Boehringer Ingelheim, Heidelberg, Germany; 0.01% final concentration in 0.1% acetic acid) before the cells were seeded at a concentration of 10^4 cells/ml. Experiments were performed 3 d later when the cells formed a confluent monolayer according to light microscopic examination. Routinely, 0.5 ml of fluid was kept in the upper chamber and 1.5 ml in the lower.

Monolayers were infected for 2 h in the upper chamber with 500 μl of a 10^7 CFU/ml suspension. Throughout these experiments, lactate dehydrogenase (LDH) release was measured as described in detail below to confirm that no cell injury occurred at any time. After 2 h the monolayer was washed three times and antibiotic-containing medium (10 μg/ml penicillin G, 200 μg/ml gentamicin) was added to both chambers for 1 h to kill extracellular organisms. Control monolayers were lysed to determine the number of intracellular bacteria. The remaining monolayers were washed three times again and antibiotic-containing medium (DME + 10% FBS + 0.04 μg/ml penicillin G) was added to the upper chamber (for transcytosis assays) or the lower chamber (for recycling assays). These concentrations were sufficient to maintain these chambers sterile throughout the experiment (2× MIC for P125 and 4× MIC for P126). This was done in order to avoid any interference of replicating extracellular bacteria in these chambers with the measurement of viable counts in the other chamber. The lower chamber (in transcytosis assays) or the upper chamber (in recycling assays) was filled with antibiotic-free medium (DME + 10% FBS). The antibiotics maintained in the corresponding chambers did not diffuse across the monolayer in significant amounts as evidenced by bacterial growth during the experiment and viable counts could be performed in the lower chamber (transcytosis assays) or upper chamber (recycling assays).

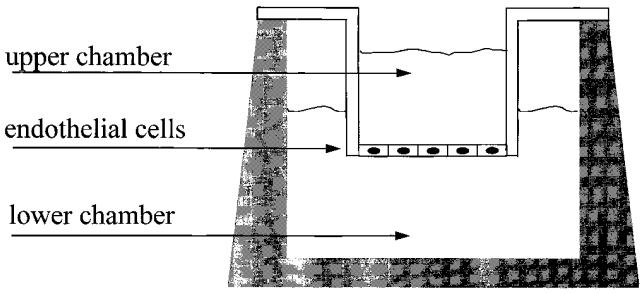

Figure 1. Schematic diagram of the two-chamber culture system used to grow monolayers of BMEC. A monolayer covers the collagen-coated polycarbonate membrane (surface area ~ 1 cm^2, containing 12-μm pores) and is bathed in culture medium above and below. Cells form a confluent monolayer within 3 d after initial seeding at 5×10^4 cells/well. Fluid in the upper chamber is in contact with the apical surface of the cells, and fluid in the lower chamber has access to the basal surface.

Assay for endothelial cell injury. Endothelial cell injury was assessed by exclusion of trypan blue (0.2% in DME) and the release of LDH activity into the culture medium at various time points ranging from 2 to 22 h after inoculation. Trypan blue exclusion was quantified by counting 100 cells per well using inverted phase-contrast microscopy. The LDH activity in cell culture media and cell lysates was determined by a colorimetric assay (Sigma Chemical Co., St. Louis, MO) for pyruvate with the amount of residual pyruvate being inversely proportional to the amount of LDH activity. The total LDH activity was measured in quadruplicate wells in which the monolayers were lysed with 0.025% Triton X-100. The LDH release is presented as the ratio of LDH activity in experimental wells to wells containing cell lysates in the same volume. Experiments were performed three times and each condition was assessed in quadruplicate.

Acridine orange and ethidium bromide (Sigma Chemical Co.) were used to assess cell viability morphologically using fluorescent microscopy. Acridine orange stains DNA bright green in viable cells. Ethidium bromide stains DNA orange but is excluded by viable cells (20). Both agents were used at a final concentration of 10 μg/ml to stain monolayers that were viewed with a fluorescein filter.

Inhibitors of invasion. The PAF-Ra L659,989 (trans-2-[3-methoxy-5-methylsulfonyl-4-propoxyphenyl]-5-[3,4,5-trimethoxyphenyl] tetrahydrofuran; Merck Sharp & Dohme Research Laboratories, Rahway, NJ) is a competitive antagonist of the receptor for PAF (21). It functionally blocks human and rat PAF receptors, which share a 79% homology (22). It has been shown previously to inhibit adherence and invasion of *S. pneumoniae* to peripheral endothelial cells and lung epithelial cells in vitro and in vivo (6). It was dissolved at a concentration of 50 mM (26 μg/ml) in DMSO and then further diluted 1:1,000 in DME + 10% FBS at 37°C. The final concentration used to pretreat BMEC monolayers for 15 min before inoculation of bacteria was 12 μg/ml. All control wells used in the experiments involving L659,989 were treated with 0.05% DMSO to ensure that DMSO treatment did not interfere with cell function.

Cytochalasin D, an inhibitor of actin polymerization, and nocodazole, an inhibitor of microtubule formation, were purchased from Sigma Chemical Co. and dissolved in DMSO.

Viability of BMEC was determined at the end of each experiment by trypan blue exclusion and in every case was > 99%.

Electron microscopy. BMEC monolayers were infected with midlog phase *S. pneumoniae* cultures resuspended in DME + 10% FBS at a concentration of 10^7 CFU/ml in 25-cm^2 cell culture flasks. After 2 h, monolayers were washed in DME without serum and fixed on ice in 0.5% glutaraldehyde in 0.1 M cacodylate buffer, pH 7.4, and subsequently stored in 2% glutaraldehyde. Monolayers were then washed in buffer and postfixed for 1 h in 1% OsO_4 in cacodylate buffer, then stained with 0.5% aqueous uranyl acetate at room temperature for 1 h, and dehydrated through a graded ethanol series. The BMEC were then treated with propylene oxide, embedded in Epon, and thin sectioned. Sections were collected on Carbon-Formvar coated copper grids and stained in uranyl acetate and lead citrate before viewing in a JEOL 1200 EX II electron microscope operated at 80 kV.

Results

Time course, dose dependence, and ultrastructure of BMEC invasion. Adherence of *S. pneumoniae* to BMEC reached saturation within the first 30 min of coincubation (Fig. 2). In contrast, penetration of the cells by the bacteria as assessed by protection from extracellular antibiotic was a delayed process

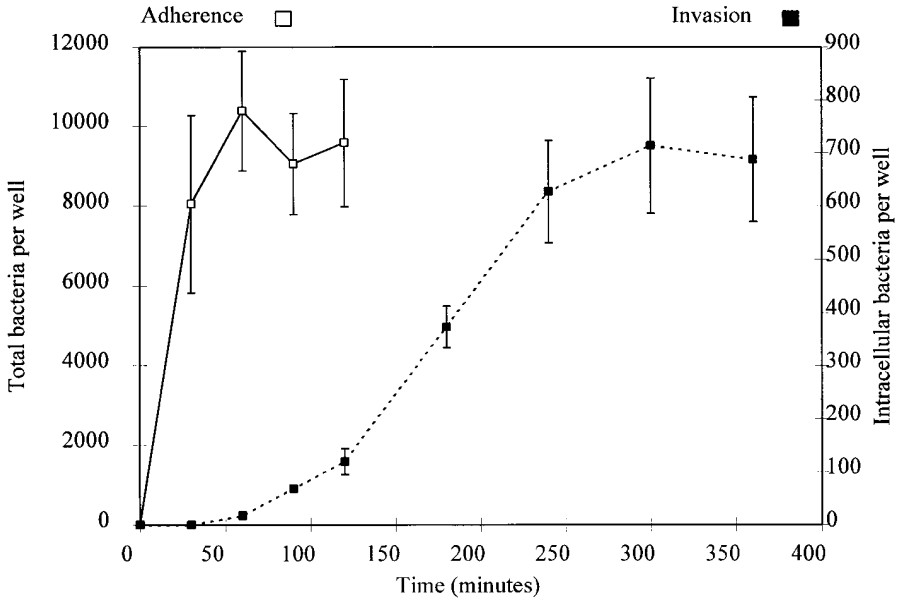

Figure 2. Kinetic parameters of *S. pneumoniae* type 9V strain P383 adherence and invasion of rat BMEC. The total number of extracellular plus intracellular bacteria (*open boxes; left axis*) was quantitated in lysates of washed confluent BMEC monolayers challenged with 10^7 *S. pneumoniae*. The number of intracellular bacteria (*filled boxes; right axis*) was determined by quantitating CFU surviving extracellular penicillin/gentamicin treatment.

that was initiated during the second hour after incubation and which reached a plateau between 4 and 5 h (Fig. 2).

A linear correlation between the number of eukaryotic cells and the number of adherent and intracellular bacteria was documented at an moi between 30 and 150 ($1–5 \times 10^7$ CFU/ml). At a higher moi, cell damage became evident beyond 5 h of incubation as assessed by increased release of LDH and separation of cells forming a confluent monolayer, while lower moi resulted in decreased invasion efficiency (not shown).

Transmission electron microscopy studies were performed to confirm the intracellular location of pneumococci. As shown in Fig. 3, intracellular pneumococci are found in intracellular vesicles. Transmission electron microscopy was also suitable to confirm the integrity of BMEC during experiments.

Invasiveness of various clinical isolates. 13 encapsulated clinical *S. pneumoniae* isolates from blood or cerebrospinal fluid belonging to 7 serotypes were screened for the capacity to penetrate rat BMEC in vitro. Table I shows the number of intracellular bacteria determined after incubating the BMEC for 2 h with 10^7 CFU/ml. The ability to invade brain endothelia varied significantly between different isolates ranging from 2 to 846 CFU/well. This was independent of serotype. For two isolates, spontaneous nonencapsulated variants were also tested and the presence of a polysaccharide capsule appeared to significantly attenuate the ability to invade BMEC (Table

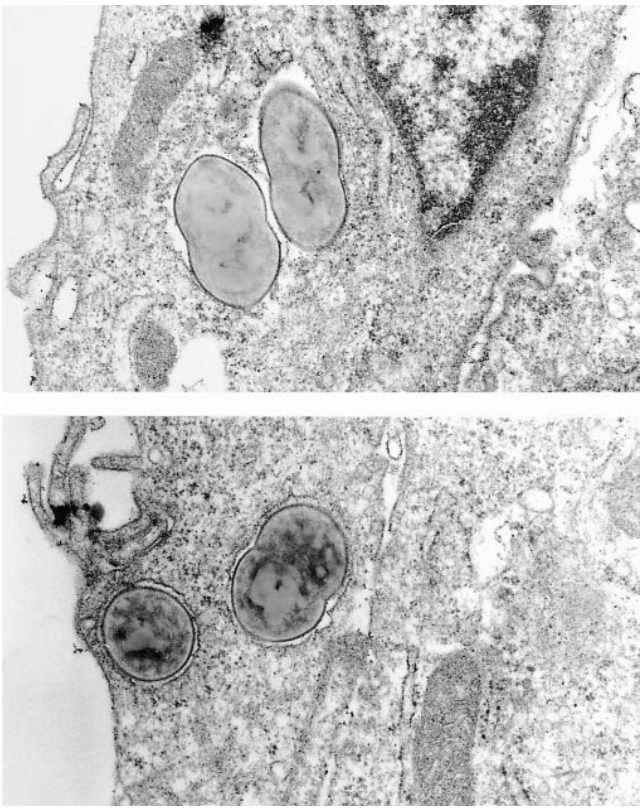

Figure 3. Transmission electron micrographs of intracellular *S. pneumoniae* in a rat BMEC vacuole at a magnification of 36,000.

Table II. Invasiveness of Nonencapsulated S. pneumoniae Strains

Isolate	Intracellular bacteria per well
P284 (type 7F)	107±36
P285 (nonencapsulated)	18100±8000
P397 (type 1V)	61±17
P395 (nonencapsulated)	14100±7100
R6x (nonencapsulated)	15900±4200
P125 (opaque, nonencapsulated)	15700±678
P126 (transparent, nonencapsulated)	13500±643

Rat BMEC monolayers were infected with 10^7 *S. pneumoniae* per well for 2 h and quantitative cultures were grown after antibiotic killing of adherent CFU and lysis of the cells. P285 and P395 are spontaneous nonencapsulated derivatives of originally encapsulated clinical isolates (P284 and P397, respectively).

Table III. Comparison of Surface Characteristics of Opaque (O) and Transparent (T) Variants with Rat BMEC Adherence and Invasion

T/O pair	Capsular polysaccharide	Teichoic acid	Adherence	Invasion
P71/73	0.83	2.1	5.3	6.2
P382/383	0.18	ND	2.9	4.3
P376/384	0.42	3.8	2.8	*

The values presented are transparent/opaque ratios. Capsular polysaccharide and teichoic acid were quantitated by a sandwich ELISA as stated in reference 9. Adherence was assessed by infecting with 10^7 bacteria per well and incubating for 30 min followed by washing and quantitation of colony-forming units in cell lysates. For invasion assays, rat BMEC were incubated with bacteria for 2 h, treated with antibiotics, washed, and then lysed for quantitative culture. *Invasion was too low to give adequate data.

II). The average number of intracellular bacteria for five nonencapsulated strains was 15,460±1,800 CFU/well, a value 2 to 3 logs greater than the invasion recorded for the corresponding encapsulated variants.

For seven clinical isolates, opaque and transparent phase variants were available. Transparent phenotypes were more invasive for all pairs tested, a difference reaching statistical significance for five of seven strains (Table I). Quantitation of capsular polysaccharide and teichoic acid by a sandwich ELISA assay on three of these pairs revealed that for each pair, transparent variants had less capsular material and more teichoic acid than their opaque counterparts (Table III). There was only a relatively small difference in invasiveness between opaque and transparent variants of the nonencapsulated strain R6 (P125 and P126, Table II). These findings raise the possibility that the amount of capsular polysaccharide is a critical factor in levels of invasiveness.

Inhibitors of cytoskeletal function. To investigate if pneumococcal uptake into brain endothelial cells requires functional microfilaments or microtubules, the capacity of P126 (a transparent phase variant of R6) to penetrate cells pretreated with cytochalasin D (an inhibitor of actin polymerization) or nocodazole (an inhibitor of microtubule aggregation) was determined. Exposure of the cells to nocodazole decreased invasion by ~60% in human BMEC and 75% in rat BMEC (Fig. 4 *A*) at 10 μM, the highest concentration not causing cell injury. Cytochalasin D totally abrogated invasion of human and rat BMEC at concentrations > 0.5 μg/ml (Fig. 4 *B*). Thus, pneumococcal invasion of BMEC is dependent on microtubules as well as microfilaments.

Involvement of choline in BMEC cell invasion. Phosphorylcholine is an unusual and predominant cell wall component of *S. pneumoniae*. Since choline has been suggested to be in-

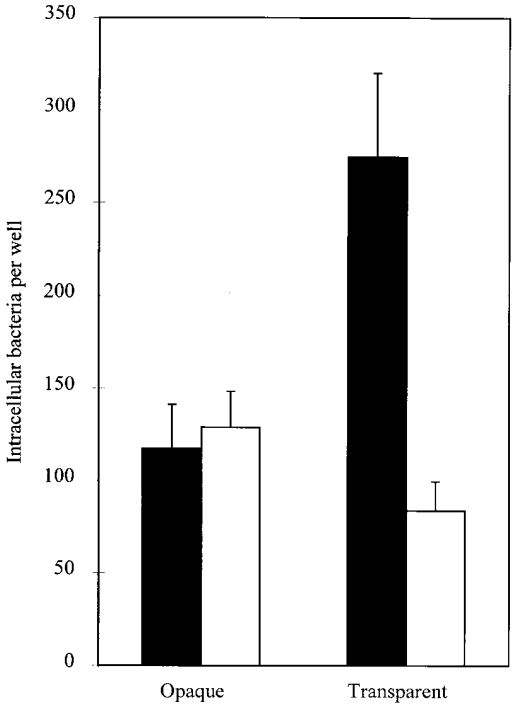

Figure 5. Invasion of rat BMEC by the type 9V *S. pneumoniae* strains P62 (*Opaque*) and P64 (*Transparent*) grown in the synthetic medium C_{den} containing either choline (*filled boxes*) or ethanolamine (*open boxes*).

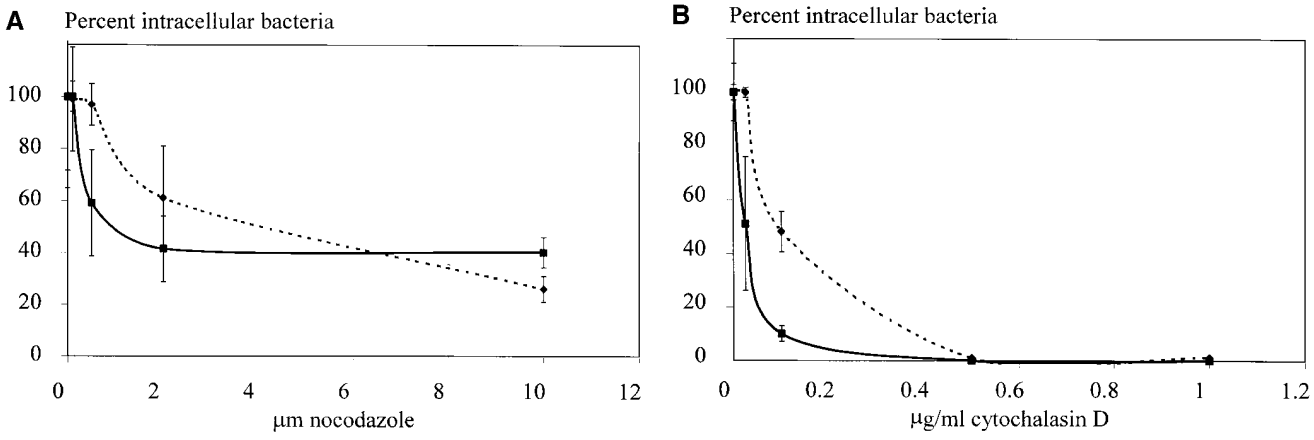

Figure 4. Dose-dependent influence of nocodazole (*A*) and cytochalasin (*B*) on invasion of rat (*dashed lines*) and human (*solid lines*) BMEC monolayers.

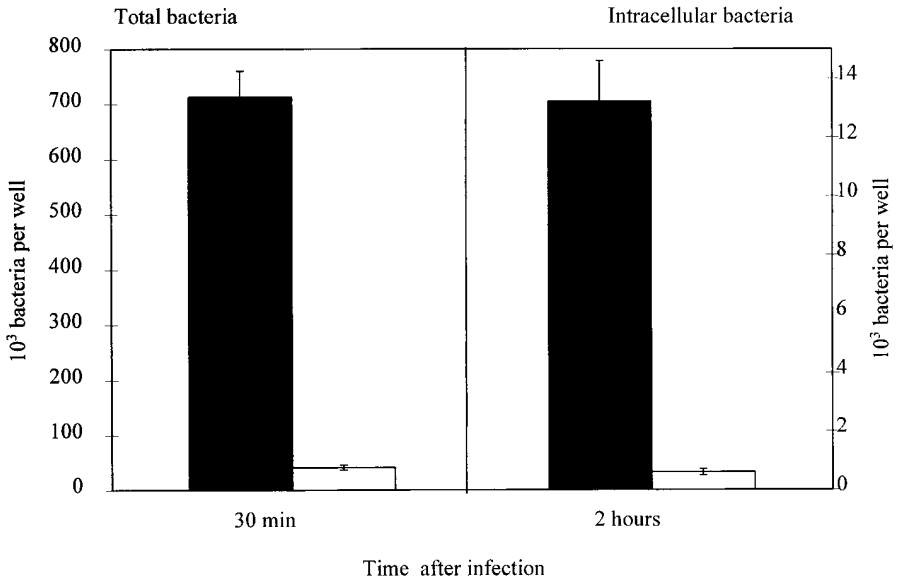

Figure 6. Adherence and invasion of rat BMEC by a mutant deficient in CbpA (*open boxes*) and the parental strain R6x (*filled boxes*). (*Left*) The total number of adherent and intracellular bacteria after 30 min of infection. (*Right*) The number of intracellular bacteria after 2 h of infection and subsequent antibiotic killing of extracellular bacteria.

volved in adherence and invasion of peripheral eukaryotic cells by pneumococci, and since the transparent variants that adhere and penetrate BMEC more efficiently also have more choline-containing teichoic acid incorporated into their cell wall, the effect of replacing cell wall choline by ethanolamine was tested. As demonstrated in Fig. 5, growth in ethanolamine-containing medium decreased the invasiveness of the transparent variant (P64, a type 9V strain) to the basal levels of the opaque (P62) phase variant. No effect on invasion by opaque variants was found.

The effect of choline on invasion could arise by its action as a direct ligand for human cells or indirectly through presentation of adhesive Cbps. To investigate the second possibility, a mutant defective in the production of the known adhesin CbpA was tested for adherence and invasion of rat BMEC. Adherence and invasion of the mutant were decreased 95% compared with the parental strain R6x (Fig. 6), indicating the importance of this protein in the interaction of pneumococci with brain endothelium. A mutant defective in production of another Cbp, the autolysin, was tested as a control and demonstrated adherence and invasion similar to the wild type.

The direct action of choline in the binding of pneumococci to human cells has been postulated to involve ligation of the PAF receptor. To determine if this was operative on brain endothelium, TNF-α–activated and resting BMEC were pretreated with the PAF-Ra L659,989 15 min before challenging the monolayers with pneumococci. Activation of human BMEC with TNF-α (10 ng/ml, 3 h) results in increased invasion of transparent (44%, Fig. 7 *A*) and opaque pneumococci (28%, Fig. 7 *B*). PAF-Ra decreased invasion of transparent

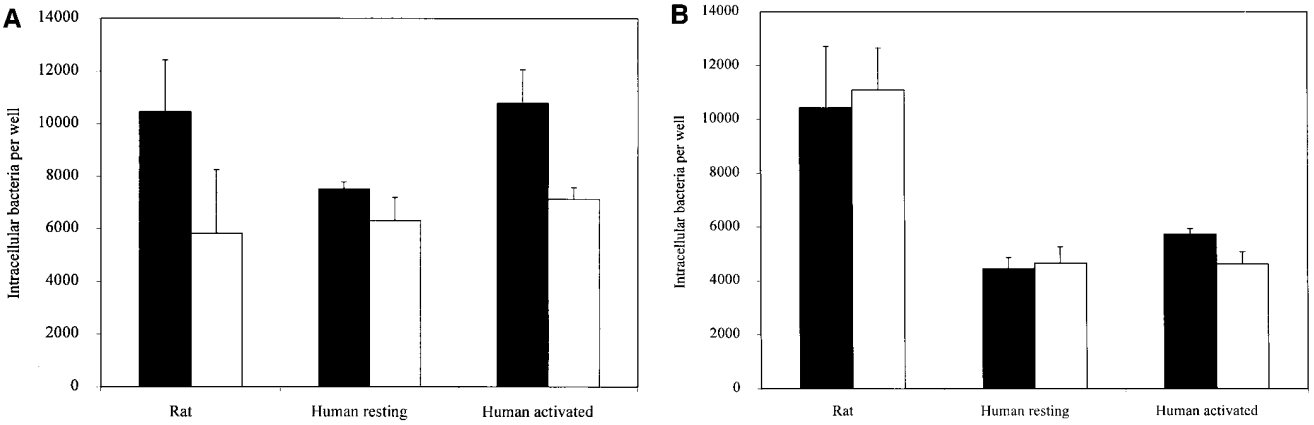

Figure 7. Influence of the PAF-Ra on BMEC invasion. Human BMEC were activated with TNF-α (10 ng/ml) for 3 h before the experiment. Rat and human BMEC monolayers were pretreated with the PAF-Ra 15 min before infection of the monolayers with transparent (*A*) and opaque (*B*) phase variants of the nonencapsulated *S. pneumoniae* strain R6. Invasion assays were then performed for 2 h followed by antibiotic treatment to kill extracellular pneumococci and quantitative culture of intracellular bacteria. Data are means and standard deviations for quadruplicate wells. *Filled boxes*, control; *open boxes*, PAF-Ra–treated cells. The *P* values for the differences of invasion of rat and activated human BMEC by the transparent phase variant indicated statistical significance (< 0.05).

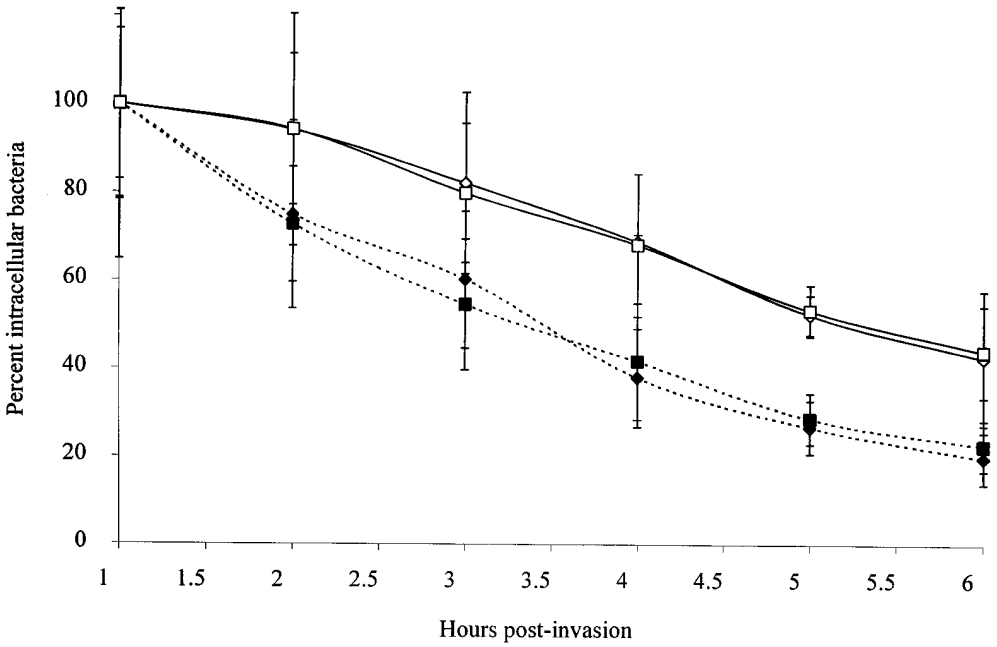

Figure 8. Viability of intracellular bacteria after invasion. Rat (*dashed lines*) and human (*solid lines*) BMEC monolayers were infected with the opaque variant P125 (*diamonds*) and the transparent counterpart P126 (*squares*) and were subjected to the 2-h invasion assay followed by treatment with penicillin and gentamicin for the time periods indicated on the *x* axis. Cells were then washed and lysed and aliquots plated on blood agar to determine the number of intracellular bacteria. Data are means±standard deviations.

phase variants by 35% in activated and 15% in resting human BMEC (Fig. 7 *A*), suggesting that PAF receptors are upregulated by cytokine activation. Invasion by opaque forms is inhibited less by PAF-Ra (20% in activated cells, no inhibition in resting, Fig. 7 *B*), which was expected if opaque forms have less choline than transparent. In rat BMEC, TNF-α treatment did not alter pneumococcal invasion or inhibition by L659,989. However, the PAF-Ra–mediated inhibition of transparent invasion amounted to 40% in untreated cells (Fig. 7 *A*), which is more similar to activated than resting human BMEC.

Postinvasion trafficking of pneumococci. To assay survival of intracellular pneumococci, bacteria were allowed to invade BMEC monolayers for 2 h, extracellular bacteria were eliminated both by washing the monolayer and by addition of antibiotics to the medium (sufficient to kill the entire inoculum in 1 h), and surviving bacteria were quantified over time in cell lysates. Over 6 h, the number of viable intracellular pneumococci decreased continuously to ~ 45% of the initial value in human and ~ 20% in rat BMEC (Fig. 8). There was no appreciable difference in the rate of loss between opaque and transparent variants.

Table IV. Quantitation of Cell Damage during Invasion

Hours after invasion	No bacteria	With bacteria
2	1.7±0.03%	2.0±0.02%
3	1.8±0.04%	1.6±0.03%
10	2.3±0.07%	1.5±0.06%
20	3.0±0.09%	2.3±0.02%

Rat BMEC were subjected to the 2-h invasion assay, and LDH activity released was quantitated at the indicated times. Antibiotics were maintained in the media for 20 h; controls were not treated with bacteria. 100% refers to the LDH activity in cell culture media of monolayers lysed with Triton X-100 at time 0. All data are means±standard deviations of quadruplicate wells.

A decrease in recoverable intracellular bacteria could reflect killing by the host cell or exocytosis from the cell. To determine whether intracellular pneumococci were released from the apex or basolateral aspect of the cell after invasion, polarized rat and human BMEC monolayers separating two chambers were loaded with intracellular bacteria by a 2-h challenge of the upper chamber followed by antibiotic treatment in both chambers. Subsequently, fresh medium without antibiotic was placed in the chamber to be studied. To rule out bacterial release due to cell damage, trypan blue exclusion by the cells and LDH activity in the assay medium were measured. An example is given in Table IV. There was no indication of injury to the cells mediated by intracellular pneumococci even over periods of 20 h. Trypan blue exclusion showed that cells were > 99% viable throughout this period. In addition, acridine orange/ethidium bromide staining to differentiate between viable and nonviable cells was performed using fluorescent microscopy. This protocol confirmed that the adherent BMEC in the monolayers were > 99.9% viable up to 6 h after invasion in the transcytosis experiments. Measurement of the TEER demonstrated stable values for at least 14 h after invasion, suggesting that pneumococci did not compromise tight junctions (Table V). Thus, invasion of BMEC by pneumococci did not

Table V. TEER across Polar Human BMEC Monolayers during Transcytosis Experiments ($\Omega \times cm^2$)

	Opaque	Transparent
Before experiment	186±8	206±11
After antibiotic killing	200±11	224±10
4 h after invasion	194±10	218±11
14 h after invasion	201±13	231±13
22 h after invasion	153±7	168±11

Monolayers were treated as described in Fig. 9, but the period of observation after the antibiotic killing step was extended up to 22 h.

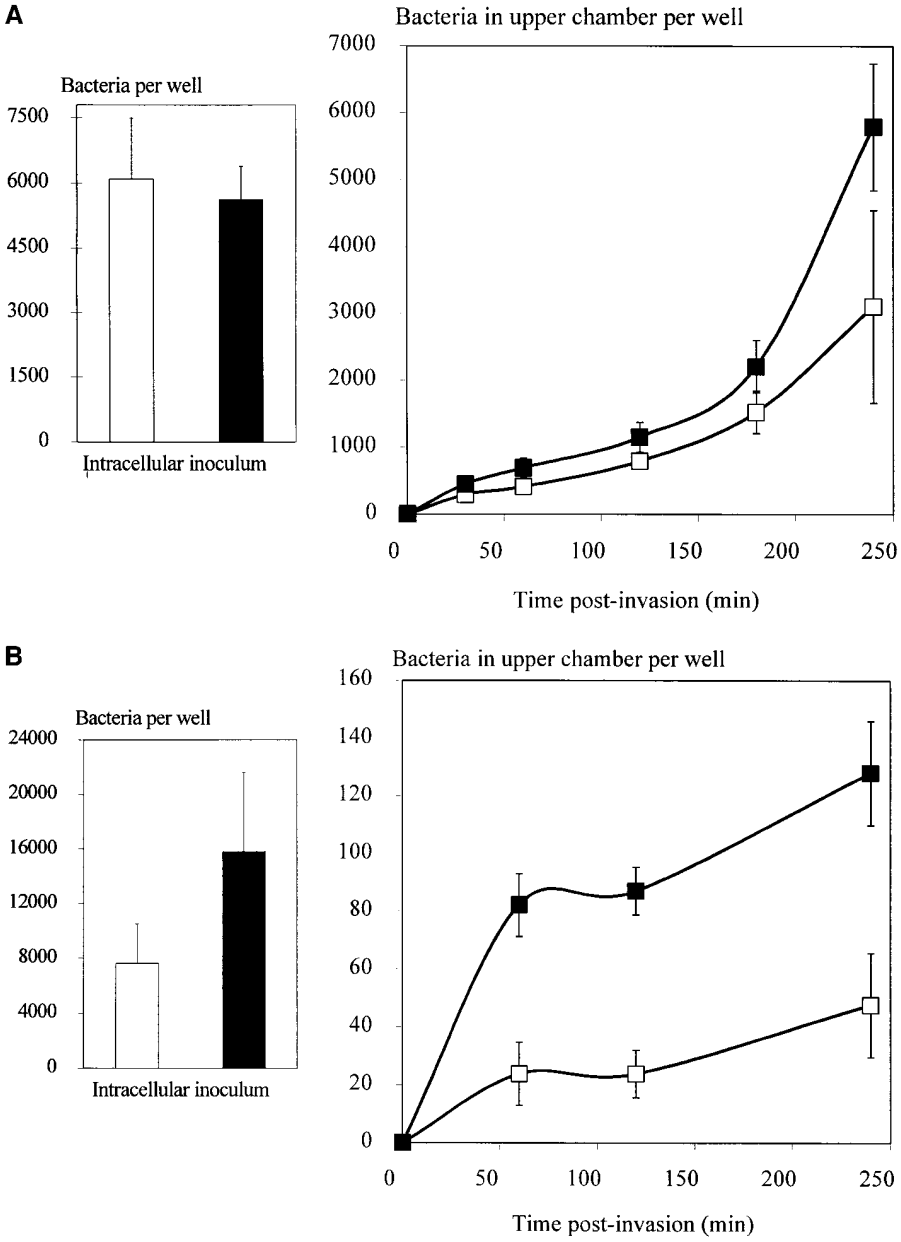

Figure 9. Recycling and transcytosis of intracellular pneumococci. *S. pneumoniae* P125 (opaque) (*open boxes*) and P126 (transparent) (*filled boxes*) were allowed to invade human or rat BMEC monolayers from the upper chamber and extracellular bacteria remaining at 2 h were killed by antibiotics. The monolayers were washed and antibiotic-free medium was added to the upper chamber (*A*, rat; *B*, human BMEC) or to the lower chamber (*C*, rat; *D*, human BMEC). The opposite chamber was filled with antibiotic-containing medium. Aliquots of the medium in the upper chamber (*A* and *B*) or lower chamber (*C* and *D*) were removed after the time periods indicated and quantitatively cultured to determine the number of bacteria. The antibiotic-containing chamber remained sterile throughout the experiment. The bar diagram shows equivalent intracellular bacterial concentrations at time 0 for opaque and transparent phase variants. Data are means±standard deviations. The differences between opaque and transparent were statistically significant ($P < 0.05$) at all time points.

result in parameters indicative of injury to cells or intercellular junctions, suggesting that the appearance of bacteria observed in the medium was most likely due to exocytosis of viable pneumococci from within intact BMEC.

Fig. 9 shows the increasing numbers of extracellular bacteria in the upper and lower chamber arising from previously intracellular organisms. Since the number of extracellular bacteria in this assay system depends on the rate of exocytosis as well as bacterial replication in the assay medium, we confirmed that the generation time was identical for opaque and transparent bacteria (data not shown). The number and percentage of transparent pneumococci recycling from the intracellular compartment back into the apical chamber was much higher in rat than in human BMEC (Fig. 9, *A* and *B*). However, the difference between phase variants was comparable: transparent recycle approximately twofold more out of rat BMEC (Fig. 9 *A*) and fourfold more out of human BMEC (Fig. 9 *B*) throughout the measurement period. Taking into account that invasion of human BMEC by transparent forms was already increased twofold (Fig. 9 *B*), recycling relative to the intracellular load was altogether twofold more effective in transparent phase variants. In rat BMEC, this recycling back to the original entry surface was detectable as soon as 30 min after entry into the cell, a time when very few bacteria appeared in the lower chamber.

The capability of transparent variants to transcytose through BMEC exceeded that of the opaque more than 10-fold in rat (Fig. 9 *C*) and human BMEC (Fig. 9 *D*). Virtually no opaque bacteria exited into the lower chamber. Like recycling, transcytosis is numerically less in human compared with rat BMEC. Although eventually a numerically dominant route, the number of transparent bacteria in the lower chamber was not sub-

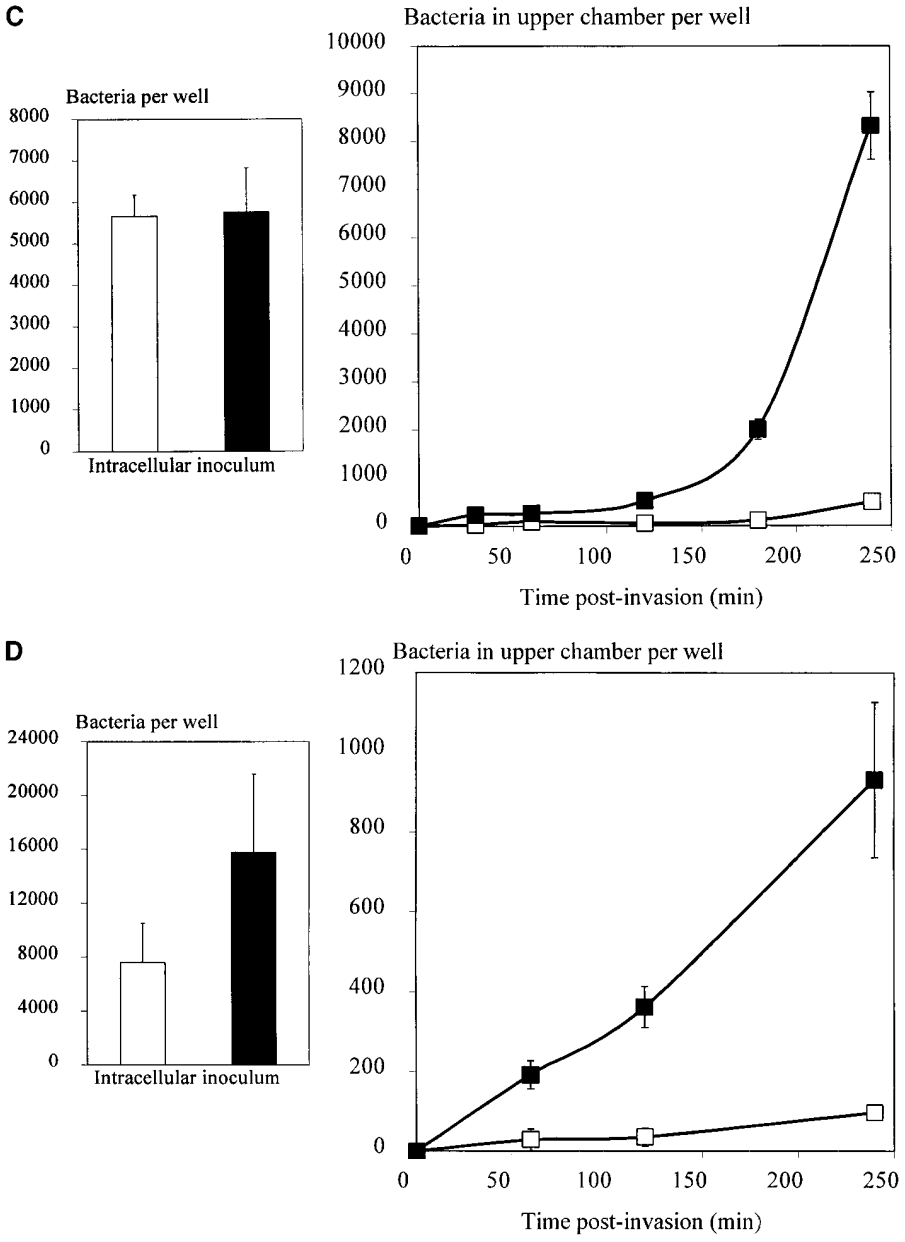

Figure 9 (Continued)

stantial until 120 min after the antibiotic killing step, i.e., 5 h after bacterial inoculation into the upper chamber. Thus, given sufficient time, intracellular transparent bacteria preferentially translocated vectorially across the monolayer emerging on the cell surface opposite to their entry.

In summary, transparent intracellular pneumococci appear to transcytose to the basal side and recycle back to the apical surface as viable bacteria, whereas opaque bacteria undergo some recycling while the majority dies.

Influence of PAF-Ra on trafficking of pneumococci. The fate of intracellular pneumococci appeared to be different for opaque and transparent phase variants. Since the transparent phenotype had demonstrated PAF-Ra–sensitive invasion, we sought to determine whether the PAF receptor was also differentially involved in translocation versus recycling of the transparent phase variant P126. Rat and TNF-α–activated human BMEC monolayers pretreated with PAF-Ra and controls were subjected to the standard invasion assay. After killing all extracellular bacteria, the percentages of bacteria exiting from the intracellular compartment into either the lower or upper chamber were determined. In addition to the 35% decrease of the intracellular bacterial load in the PAF-Ra–treated monolayers (rat and human BMEC, Tables VI and VII), the relative amount of transcytosis (i.e., the transcytosis to invasion ratio) was an additional 25% (human BMEC, Table VII) to 30% (rat BMEC, Table VI) decreased at all time points, suggesting that the absence of functional PAF receptor decreases transcytosis in excess of invasion. In contrast, the relative number of bacteria being recycled to the apical surface was increased $\sim$ 40% in the absence of functional PAF receptor (rat BMEC, Table VIII). In human BMEC, recycling was generally low but relative to the intracellular load approximately threefold higher in

Table VI. Rat BMEC: Percent Transmigration to the Lower Chamber

Rat BMEC	Intracellular bacteria per well		Percent of intracellular bacteria appearing in the lower chamber after removal of antibiotics in the medium		
			1 h	2 h	3 h
Control	6635±1031	Mean±SD	9.7*±2.1	24*±3.1	51±7.1
		Median	9.6	24.1	51.2
		Range	6.5–12.7	19.8–28.1	39.3–61.6
		TEER ($\Omega \times cm^2$)	128±7	126±7	128±8
PAF-Ra	4287±1219	Mean±SD	6.6*±1	17.6*±5.2	35.8±16.6
		Median	6.3	18.5	39.3
		Range	5.6–8.2	9.6–23.6	14.1–55.3
		TEER ($\Omega \times cm^2$)	122±7	119±6	123±7

Influence of the PAF receptor antagonist on pneumococcal recycling and transcytosis in rat BMEC. The monolayers were pretreated with PAF-Ra or culture medium alone and challenged with transparent pneumococci in the upper chamber. After 2 h, extracellular bacteria were killed with antibiotics (time point 0 h). The number of extracellular CFU appearing in the indicated chamber was assessed in quadruplicate by quantitative cultures. The differences between controls and PAF-Ra–treated cells were analyzed by Student's *t* test (two-tailed). $*P < 0.05$. The baseline values were: control = 129±7, PAF-Ra = 124±6.

PAF-Ra–treated cells (Table IX). In summary, transparent pneumococci entering a cell by engaging the PAF receptor might preferentially traffic across the cell and exit the basal side of BMEC.

Discussion

S. pneumoniae has been shown to bind to and invade peripheral endothelial and epithelial cell monolayers in a receptor-dependent fashion (6, 19, 23). The biology of this process in vitro has been shown to be predictive of factors involved in the development of bacteremia after pneumonia in animal models. However, relevance of this mechanism to egress of bacteria from the bloodstream into tissues in meningitis is untested. Meningitis due to *S. pneumoniae* develops during high-grade bacteremia in relatively few individuals. Thus, it is not clear if meningeal invasion is simply a matter of statistical chance or if there exists a specific mechanism for pneumococcal targeting of the BBB that may or may not bear a relationship to transmigration across peripheral endothelia. Also, it is unknown if the organisms primarily invade the central nervous system at a preferred anatomical site of the BBB. Theoretically, the initial site of entry could be the endothelial BBB as well as the choroid plexus epithelium or sites in the brain where the barrier is not complete such as the circumventricular organs. In this study we chose to investigate the endothelial BBB because it covers the largest surface area of the BBB and thus allows extensive targeting by blood-borne bacteria (24). Transit of bacteria across the endothelial BBB is conceivable either via a transcellular or a paracellular pathway, the latter of which would include compromising the tight junctions. Since we did not find evidence for paracellular migration in electron microscopy studies, we focused on transcellular migration in this study. Evidence for a specific transcytotic mechanism would offer potential avenues to control this devastating infection. We demonstrate here that pneumococci are capable of pene-

Table VII. Activated Human BMEC: Percent Transmigration to the Lower Chamber

Activated human BMEC	Intracellular bacteria per well		Percent of intracellular bacteria appearing in the lower chamber after removal of antibiotics in the medium		
			1 h	2 h	3 h
Control	19134±4033	Mean±SD	4.33*±0.53	4.95±1.16	7.12±2.06
		Median	4.43	4.33	6.09
		Range	3.71–4.64	4.23–6.29	5.78–9.49
		TEER ($\Omega \times cm^2$)	197±11	193±7	194±11
PAF-Ra	12256±3232	Mean±SD	3.33*±1.3	4.03±1.68	5.07±1.43
		Median	2.98	3.13	4.48
		Range	2.24–4.78	2.99–5.97	4.03–6.72
		TEER ($\Omega \times cm^2$)	199±11	196±10	188±10

Influence of the PAF receptor antagonist on pneumococcal recycling and transcytosis in human BMEC. The monolayers were pretreated with PAF-Ra or culture medium alone and challenged with transparent pneumococci in the upper chamber. After 2 h, extracellular bacteria were killed with antibiotics (time point 0 h). The number of extracellular CFU appearing in the indicated chamber was assessed in quadruplicate by quantitative cultures. The differences between controls and PAF-Ra–treated cells were analyzed by Student's *t* test (two-tailed). $*P < 0.05$. The baseline values were: control = 195±8, PAF-Ra = 194±6.

Table VIII. Rat BMEC: Percent Recycling to the Upper Chamber

Rat BMEC	Intracellular bacteria per well		Percent of intracellular bacteria appearing in the upper chamber after removal of antibiotics in the medium		
			1 h	2 h	3 h
Control	5315±1255	Mean±SD	7.3*±0.6	8.2*±0.3	8.3*±1.6
		Median	7.1	8.2	8.2
		Range	6.7–8.2	7.8–10.3	6.3–10.3
		TEER ($\Omega \times cm^2$)	134±6	136±6	138±7
PAF-Ra	2740±515	Mean±SD	10.3*±0.8	11.8*±0.3	13.8*±0.9
		Median	10	11.7	13.5
		Range	9.7–11.1	11.5–12	13.1–14.8
		TEER ($\Omega \times cm^2$)	133±7	132±7	133±9

Influence of the PAF receptor antagonist on pneumococcal recycling and transcytosis in rat BMEC. The monolayers were pretreated with PAF-Ra or culture medium alone and challenged with transparent pneumococci in the upper chamber. After 2 h, extracellular bacteria were killed with antibiotics (time point 0 h). The number of extracellular CFU appearing in the indicated chamber was assessed in quadruplicate by quantitative cultures. The differences between controls and PAF-Ra–treated cells were analyzed by Student's *t* test (two-tailed). $*P < 0.05$. The baseline values were: control = 132±7, PAF-Ra = 137±7.

trating rat and human BMEC in vitro. The properties of this process indicate it is specific and receptor mediated. The rat and human BMEC used in this study circumferentially express the tight junction–associated protein ZO-1 and enrich filamentous actin in their cell borders (not shown). They also develop significantly higher TEER than peripheral endothelial cells. These characteristics are typical for polarized epithelial and endothelial cells expressing tight junctions and are useful to distinguish between such cells that maintain apical-to-basal polarity and those that do not (25). The specialized endothelial cells that form the dominant part of the BBB resemble intestinal and kidney epithelial cells in this respect (26). The presence of these characteristics plus the markers of endothelial and cerebral origin show that this in vitro system is able to recapitulate the in vivo properties of brain microvascular endothelium and the associated BBB.

Invasion requires prior adherence of the bacteria to the surface of BMEC, a step requiring the pneumococcal adhesin CbpA. Internalization lags behind adherence temporally suggesting an invasion process involving at least two steps. The degree of invasion varies in a linear fashion with the dose of the challenge inoculum and is saturable. A maximum of ~ 7% of the adherent bacterial population becomes intracellular in rat and human BMEC. These features are suggestive of a specific internalization mechanism. Relative to peripheral vessels, it appears that pneumococci are approximately twofold more efficient at invasion of cerebral as compared with peripheral endothelial cells (data not shown).

Comparison of invasion by a variety of encapsulated clinical isolates from pediatric wards indicated that efficiency of invasion was a widely variable trait ranging from 2 to > 800 bacteria per monolayer. One factor playing prominently in invasive capability was the presence and amount of capsular polysaccharide. Spontaneous nonencapsulated variants of clinical isolates demonstrated up to 200-fold greater invasion of BMEC than isogenic encapsulated strains. Interference with

Table IX. Activated Human BMEC: Percent Recycling to the Upper Chamber

Activated human BMEC	Intracellular bacteria per well		Percent of intracellular bacteria appearing in the upper chamber after removal of antibiotics in the medium		
			1 h	2 h	3 h
Control	15237±831	Mean±SD	0.94*±0.31	1.01*±0.31	1.12*±0.41
		Median	0.96	1.03	1.17
		Range	0.62–1.24	0.69–1.31	0.69–1.51
		TEER ($\Omega \times cm^2$)	192±10	199±10	195±7
PAF-Ra	12728±843	Mean±SD	3.45*±0.65	3.68*±0.80	3.88*±0.91
		Median	3.48	3.68	3.68
		Range	2.79–4.08	2.89–4.48	3.08–4.88
		TEER ($\Omega \times cm^2$)	193±6	186±9	189±10

Influence of the PAF receptor antagonist on pneumococcal recycling and transcytosis in human BMEC. The monolayers were pretreated with PAF-Ra or culture medium alone and challenged with transparent pneumococci in the upper chamber. After 2 h, extracellular bacteria were killed with antibiotics (time point 0 h). The number of extracellular CFU appearing in the indicated chamber was assessed in quadruplicate by quantitative cultures. The differences between controls and PAF-Ra–treated cells were analyzed by Student's *t* test (two-tailed). $*P < 0.05$. The baseline values were: control = 193±11, PAF-Ra = 193±9.

invasion by capsules of pneumococci (19) and group B streptococci (27) has been described for epithelial cells. The effect on invasion of BMEC was independent of the capsular serotype suggesting that, although capsule may generally and nonspecifically attenuate invasion, other properties of the pneumococcus determine further, specific differences in invasiveness between strains.

Pneumococci exhibit spontaneous, high frequency phase variation which greatly affects the efficiency of adherence and virulence of a given strain (8). Transparent colony variants have a selective advantage over opaque variants for adherence to human epithelial cells and establishing nasopharyngeal colonization in the infant rat (8, 28). Opaque variants survive better than transparent once in the bloodstream (9). In the case of BMEC, transparent variants of clinical isolates demonstrated a three- to fivefold enhanced ability to invade when compared with opaque variants. Transparent phase variants of nonencapsulated laboratory strains show a twofold higher invasiveness in human but not rat BMEC. Since bacteremia precedes invasion of the BBB, a high frequency of switching of the opacity phenotype from opaque (the predominant form in the bloodstream) to transparent would theoretically enhance the rate of adherence to and invasion of the BBB. This possibility could not be addressed by the multiply passaged clinical isolates studied herein. A definitive investigation of the relationship of phase switching to transmigration will require development of genetic markers for each phase and phase-locked variants.

To gain insight into the mechanism of the difference in invasion of phenotypic variants, biochemical factors known to be different between the two forms were characterized for a role in BBB transmigration (9). Opaque forms of clinical isolates have more capsular polysaccharide and less phosphorylcholine-containing teichoic acid in the cell wall. Each of these biochemical parameters independently affected adherence and invasion when manipulated artificially. For instance, loss of capsule consistently increased adherence. Phosphorylcholine on the teichoic acid was shown to be required for adherence. In addition, CbpA is more prominent on the surface of the transparent variant (11). These findings suggest that the decreased adherence and invasion by opaque phase variants may reasonably be a reflection of the sum of subtle, phase-associated variations in amounts of capsule, teichoic acid, phosphorylcholine, and adhesins on the surface of opaque compared with transparent variants.

In contrast to many gram-positive organisms that replicate intracellularly and mediate cytotoxicity (29–32), *S. pneumoniae* did not appear to readily cause cell injury and were unable to remain viable intracellularly for periods beyond a few hours. No morphological or biochemical evidence of passage between cells of a monolayer was found, consistent with previous work indicating the preferred route of transit across monolayers or bilayers to be through the cell rather than between human cells (28, 33). Similar to attachment of pneumococci to peripheral endothelial cells (23), attachment to BMEC did not invoke formation of unusual cellular protrusions, as has been seen for other invasive bacteria. Rather, adherence proceeded to internalization into a vacuole, the formation of which was apparently dependent on actin polymerization as well as microtubule formation. These characteristics are indicative of receptor-mediated endocytosis.

Tethering of pneumococci to eukaryotic cells via the G protein–coupled serpentine PAF receptor has been described for systemic endothelial cells (6). The observation that pretreatment of rat or cytokine-activated human BMEC with PAF-Ra decreased invasion by transparent phase variants by $\sim$ 40% suggests that this mechanism is also operative at the endothelial BBB. Consistent with this mechanism, choline, the natural ligand for the PAF receptor, was required on the pneumococcal surface for invasion of BMEC. In peripheral endothelial cells, the PAF receptor is subject to enhanced expression after cytokine activation of the cell and this process has been linked to enhanced pneumococcal attachment (6). Rat BMEC did not demonstrate consistent differences in invasion when resting or activated (data not shown), possibly due to the relatively high expression of PAF receptors on resting rat brain cells (34). In contrast, cytokine activation of human BMEC results in increased invasion, but the effect is less than previously reported for peripheral endothelial cells (6). The PAF receptor is known to be rapidly internalized after interaction with its natural ligand (35). Internalization of phosphatidylcholines by endocytosis has been described in animal cells (36). Pneumococci could conceivably invade the host cell in a vacuole together with the PAF receptor. Such receptor-mediated endocytosis is consistent with the demonstration that the membrane of the pneumococcal vacuole retains cell surface markers (Kavita, U., and E. Tuomanen, unpublished data). PAF receptor has been shown to play an important role in the generation of inflammation during meningitis, particularly that due to *S. pneumoniae* (37).

We sought to determine the fate of *S. pneumoniae* in intracellular vacuoles. Bacteria appeared to undergo one of three fates: death within the vacuole, transit through the cells to exit the basolateral surface, and recycling of bacteria back to the apical surface. The number of intracellular pneumococci, whether transparent or opaque, steadily declined during a 6-h period. This decline was more significant in rat (80% of the initial intracellular load) than human (55%) BMEC. In rat BMEC, 5–10% of the initial intracellular load appeared in the upper chamber (recycling pathway) within 30 min. Recycling was also present in human BMEC, although numerically less. The reason for this apparent difference between these two cell lines is unclear, but this finding is consistent with the observation that intracellular survival is higher in human BMEC (Fig. 8). However, in both human and rat BMEC the transparent variants were twice as likely as opaque variants to follow the recycling route. Transmigration of a similar number of bacteria to the lower chamber required 120 min and was observed almost exclusively for transparent variants. Taken together, these data suggest that pneumococci readily recycle to the cellular surface they entered, with a slight advantage for transparent variants. However, over time, the majority of transparent bacteria makes its way across the cell and exits the basolateral surface, a process requiring more time than recycling. Opaque bacteria appear to be largely killed intracellularly. The ability of recycled bacteria to reinitiate invasion cannot be estimated from these data. The in vivo observation that only transparent forms are able to cause invasive disease supports the present data suggesting that only transparent pneumococci possess the ability to transcytose through BMEC in a significant proportion.

While invasion of systemic endothelial and lung epithelial cells has been described, a circular recycling pathway was unanticipated. This novel trafficking pattern in which bacteria

enter and exit the same cellular surface parallels the fate of the PAF receptor, which is known to recycle from the surface to an intracellular vacuole and back to the cell surface after relaying the PAF molecule to another intracellular target (38). To validate a potential recycling pathway, loss of integrity of human cells as a mechanism of exit had to be strictly ruled out. The viability of BMEC as judged by trypan blue exclusion remained > 99% at any time point, and the level of LDH release into the medium was found to be equal to untreated controls. In addition, acridine orange/ethidium bromide fluorescence staining was used to morphologically confirm cell viability in the adherent monolayer during and after the invasion assays. Thus, pneumococci appear to be capable of bona fide recycling in and out of the same surface of a human cell. The clinical significance of this pathway is unknown but it is conceivable that recycling may serve as a holding reservoir to keep invasive competent bacteria in the local environment and sequestered from host defenses until transcytosis occurs.

The divergent fates of transparent and opaque bacteria in the two chamber model raise the hypothesis that opaque pneumococci are preferably sorted to a lethal lysosomal compartment whereas transparent variants have an additional capability that directs transcytosis through the cell and, in part, recycling back to the apical side of the cell. Given that transparent pneumococci adhere preferentially to the PAF receptor and invasion is at least partially inhibited by the PAF-Ra, the differential role of the PAF receptor in the three distinct trafficking patterns was assessed. Given the fact that pneumococcal invasion via the PAF receptor is associated with increased transmigration and correspondingly decreased recycling, it can be hypothesized that pneumococci, by as yet unexplained means, corrupt the physiological mechanism of PAF receptor recycling which occurs after discharge of the natural ligand, the PAF molecule. If pneumococci remain associated with the PAF receptor in the vesicle, this may cause the vesicle to move through the cell, rather than releasing the PAF receptor for return to the apical surface. The dramatic role of the adhesin CbpA in adherence that initiates a vacuole targeted for transcytosis suggests that this protein might in part interact with the PAF receptor and serve as a pneumococcal element driving the transcytotic mechanism. Choline-containing cell wall pieces are also suitable ligands for the PAF receptor, a feature which may underlie the increased vesicle trafficking across the BBB in animals inoculated intravenously with soluble cell wall components (39). The details of the transcytosis process remain to be established but the bidirectional trafficking of the pneumococcus represents an important potential bioprobe to investigate vectorial vesical transport across mammalian cells.

Acknowledgments

We thank Lucienne Juillerat for providing the rat BMEC cell line EC 219, for technical support, and her thoughtful suggestions. We further thank Merck Sharp and Dohme Laboratories for providing L659, 989.

This work was funded by grants AI 27913 (E.I. Tuomanen), AI 38436 (J.N. Weiser), P30CA21765 (St. Jude), and the American Lebanese Syrian Associated Charities.

References

1. Stins, M.F., N.V. Prasadarao, L. Ibric, C.A. Wass, P. Luckett, and K.S. Kim. 1994. Binding characteristics of S fimbriated *Escherichia coli* to isolated brain microvascular endothelial cells. *Am. J. Pathol.* 145:1228–1236.

2. Huang, S.H., C.A. Wass, Q. Fu, N.V. Prasadarao, M.F. Stins, and K.S. Kim. 1995. *Escherichia coli* invasion of brain microvascular endothelial cells in vitro and in vivo: molecular cloning and characterization of invasion gene ibe10. *Infect. Immun.* 63:4470–4475.

3. Prasadarao, N.V., C. Wass, J.N. Weiser, M.F. Stins, S. Huang, and K.S. Kim. 1996. Outer membrane protein A of *Escherichia coli* contributes to invasion of brain microvascular endothelial cells. *Infect. Immun.* 64:146–153.

4. Krivan, H.C., D.D. Roberts, and V. Ginsburg. 1988. Many pulmonary pathogenic bacteria bind specifically to the carbohydrate sequence GalNAc β1-4 Gal found in some glycolipids. *Proc. Natl. Acad. Sci. USA.* 85:6157–6161.

5. Andersson, B., B. Eriksson, E. Falsen, A. Fogh, L. Hanson, H. Nylen, H. Peterson, and C. Svanborg-Eden. 1981. Adhesion of *Streptococcus pneumoniae* to human pharyngeal cells in vitro. *Infect. Immun.* 32:311–317.

6. Cundell, D.R., N.P. Gerard, C. Gerard, I. Idänpään-Heikkilä, and E.I. Tuomanen. 1995. *Streptococcus pneumoniae* anchor to activated human cells by the receptor for platelet-activating factor. *Nature.* 377:435–438.

7. Cundell, D.R., J.N. Weiser, J. Shen, A. Young, and E.I. Tuomanen. 1995. Relationship between colonial morphology and adherence of *Streptococcus pneumoniae. Infect. Immun.* 63:757–761.

8. Weiser, J.N., R. Austrian, P.K. Sreenivasan, and H.R. Masure. 1994. Phase variation in pneumococcal opacity: relationship between colonial morphology and nasopharyngeal colonization. *Infect. Immun.* 62:2582–2589.

9. Kim, J.O., and J.N. Weiser. 1998. Association of intrastrain phase variation in quantity of capsular polysaccharide and teichoic acid with the virulence of *Streptococcus pneumoniae. J. Infect. Dis.* 177:368–377.

10. Weiser, J.N., Z. Markiewicz, E.I. Tuomanen, and J.H. Wani. 1996. Relationship between phase variation in colony morphology, intrastrain variation in cell wall physiology, and nasopharyngeal colonization by *Streptococcus pneumoniae. Infect. Immun.* 64:2240–2245.

11. Rosenow, C., P. Ryan, J.N. Weiser, S. Johnson, P. Fontan, A. Ortqvist, and H.R. Masure. 1997. Contribution of novel choline-binding proteins to adherence, colonization and immunogenicity of *Streptococcus pneumoniae. Mol. Microbiol.* 25:819–829.

12. Morrison, D.A., M.C. Trombe, M.K. Hayden, G.A. Waszak, and J.D. Chen. 1984. Isolation of transformation-deficient *Streptococcus pneumoniae* mutants defective in control of competence, using insertion-duplication mutagenesis with the erythromycin resistance determinant of pAM beta 1. *J. Bacteriol.* 159:870–876.

13. Lacks, S., and R.D. Hotchkiss. 1960. A study of the genetic material determining an enzyme activity in pneumococcus. *Biochem. Biophys. Acta.* 39: 508–517.

14. Juillerat-Jeanneret, L., A. Aguzzi, O.D. Wiestler, P. Darekar, and C. Janzer. 1992. Dexamethasone selectively regulates the activity of enzymatic markers of cerebral endothelial cell lines. *In Vitro Cell. Dev. Biol.* 28A:537–543.

15. Aguzzi, A., P. Kleihues, K. Heckl, and O.D. Wiestler. 1991. Cell-type specific tumor induction in neural transplants by retrovirus-mediated oncogene transfer. *Oncogene.* 6:113–118.

16. Nizet, V., K.S. Kim, M. Stins, M. Jonas, E.Y. Chi, D. Nguyen, and C.E. Rubens. 1997. Invasion of brain microvascular endothelial cells by group B streptococci. *Infect. Immun.* 65:5074–5081.

17. Tang, P., M. Foubister, M.G. Pucciarelli, and B.B. Finlay. 1993. Methods to study bacterial invasion. *J. Microbiol. Methods.* 18:227–240.

18. Isberg, R.R., and S. Falkow. 1985. A single genetic locus encoded by *Yersinia pseudotuberculosis* permits invasion of cultured animal cells by *Escherichia coli* K-12. *Nature.* 317:262–264.

19. Talbot, U.M., A.W. Paton, and J.C. Paton. 1996. Uptake of *Streptococcus pneumoniae* by respiratory epithelial cells. *Infect. Immun.* 64:3772–3777.

20. Pitrak, D.L., H.C. Tsai, K.M. McMullane, S.H. Sutton, and P. Stevens. 1996. Accelerated neutrophil apoptosis in the acquired immunodeficiency syndrome. *J. Clin. Invest.* 98:2714–2719.

21. Ponpipom, M.M., S. Hwang, T.W. Doebber, J.J. Acton, A.W. Alberts, T. Biftu, D.R. Brooker, R.L. Bugianesi, J.C. Chabala, N.L. Gamble, et al. 1988. (+/−)-trans-2-(3-Methoxy-5-methylsulfonyl-4-propoxyphenyl)-5-(3,4,5-trimethoxyphenyl)tetrahydrofuran (L-659,989), a novel, potent PAF receptor antagonist. *Biochem. Biophys. Res. Commun.* 150:1213–1220.

22. Bito, H., Z. Honda, M. Nakamura, and T. Shimizu. 1994. Cloning, expression and tissue distribution of rat platelet-activating-factor-receptor cDNA. *Eur. J. Biochem.* 221:211–218.

23. Geelen, S., C. Bhattacharrya, and E. Tuomanen. 1993. The cell wall mediates pneumococcal attachment to and cytopathology in human endothelial cells. *Infect. Immun.* 61:1538–1543.

24. Quagliarello, V.J., W.J. Long, and W.M. Scheld. 1986. Morphologic alterations of the blood-brain barrier with experimental meningitis in the rat. Temporal sequence and role of encapsulation. *J. Clin. Invest.* 77:1084–1095.

25. Pucciarelli, M.G., and B.B. Finlay. 1994. Polarized epithelial monolayers: model systems to study bacterial interactions with host epithelial cells. *Methods Enzymol.* 236:438–447.

26. Ring, A., and E. Tuomanen. 1997. Targeting bacteria to the central nervous system. *In* In Defense of the Brain. P.K. Peterson and J.S. Remington, editors. Blackwell Science, Malden, MA. 90–106.

27. Hulse, M.L., S. Smith, E.Y. Chi, A. Pham, and C.E. Rubens. 1993. Ef-

fect of type III group B streptococcal capsular polysaccharide on invasion of respiratory epithelial cells. *Infect. Immun.* 61:4835–4841.

28. Tuomanen, E.I. 1997. The biology of pneumococcal infection. *Ped. Res.* 42:253–258.

29. Gibson, R.L., M.K. Lee, C. Soderland, E.Y. Chi, and C.E. Rubens. 1993. Group B streptococci invade endothelial cells: type III capsular polysaccharide attenuates invasion. *Infect. Immun.* 61:478–485.

30. Lamont, R.J., A. Chan, C.M. Belton, K.T. Izutsu, D. Vasel, and A. Weinberg. 1995. Porphyromonas gingivalis invasion of gingival epithelial cells. *Infect. Immun.* 63:3878–3885.

31. Vann, J.M., and R.A. Proctor. 1988. Cytotoxic effects of ingested *Staphylococcus aureus* on bovine endothelial cells: role of *S. aureus* alpha-hemolysin. *Microbial Pathogenesis.* 4:443–453.

32. Bielecki, J., P. Youngman, P. Connelly, and D.A. Portnoy. 1990. *Bacillus subtilis* expressing a haemolysin gene from *Listeria monocytogenes* can grow in mammalian cells. *Nature.* 345:175–176.

33. Birkness, K.A., B.L. Swisher, E.H. White, E.G. Long, E.P. Ewing, and F.D. Quinn. 1995. A tissue culture bilayer model to study the passage of *Neisseria meningitidis. Infect. Immun.* 63:402–409.

34. Bito, H., Z. Honda, M. Nakamura, and T. Shimizu. 1994. Cloning, expression and tissue distribution of rat platelet-activating-factor-receptor cDNA. *Eur. J. Biochem.* 221:211–218.

35. Gerard, N.P., and C. Gerard. 1994. Receptor-dependent internalization of platelet-activating factor. *J. Immunol.* 152:793–800.

36. Pagano, R., and R.G. Sleight. 1984. Defining lipid transport pathways in animal cells. *Science.* 229:1051–1057.

37. Cabellos, C., D.E. MacIntyre, M. Forrest, M. Burroughs, S. Prasad, and E. Tuomanen. 1992. Differing roles for platelet-activating factor during inflammation of the lung and subarachnoid space. The special case of *Streptococcus pneumoniae. J. Clin. Invest.* 90:612–618.

38. Korth, R., and J. Benveniste. 1987. BN 52021 displaces [^{3}H]paf-acether from, and inhibits its binding to intact human platelets. *Eur. J. Pharmacol.* 142: 331–341.

39. Spellerberg, B., S. Prasad, C. Cabellos, M. Burroughs, P. Cahill, and E. Tuomanen. 1995. Penetration of the blood-brain barrier: enhancement of drug delivery and imaging by bacterial glycopeptides. *J. Exp. Med.* 182:1037–1043.